Creep rupture induced silica-based nanofibers formed on fracture surfaces of Ti_3SiC_2

Z.M. Sun[a)]
Department of Materials Science and Engineering, Drexel University, Philadelphia, Pennsylvania 19104; and National Institute of Advanced Industrial Science and Technology (AIST), Nagoya 463-8560, Japan

T.J. Zhen and M.W. Barsoum
Department of Materials Science and Engineering, Drexel University, Philadelphia, Pennsylvania 19104

(Received 21 January 2005; accepted 15 August 2005)

After creep failure at 1300 °C, silica-based nanofibers with diameters of ~250 nm and lengths of up to a few tens of microns were observed on the fracture surfaces of Ti_3SiC_2. A possible mechanism for the formation of these fibers is proposed.

Ti_3SiC_2 is a representative compound of the $M_{n+1}AX_n$ (or MAX) phases, where M is an early transition metal, A is a group-A element, X is carbon and/or nitrogen, and $n = 1–3$. By now it is fairly well established that Ti_3SiC_2 possesses good electrical conductivity ($4.3 \times 10^6\ \Omega^{-1}\ m^{-1}$) and thermal conductivity (39.9 W/mK), is relatively soft (HV 4 GPa), machinable, damage tolerant, and resistant to thermal shock.[1–6]

Because of its good high-temperature mechanical properties and oxidation resistance,[3,7,8] it is a promising candidate for high-temperature structural applications. For such applications, it is paramount to understand its creep response, which has been reported elsewhere.[9,10] The purpose of this present article, however, is not to report on its creep behavior but to report on interesting features observed on fracture surfaces of samples that were crept at 1300 °C.

Coarse-grained (grain size 30–50 μm) Ti_3SiC_2 cylinders (9.8 mm in diameter and 31 mm long) were loaded under a compressive stress of 100 MPa at 1300 °C in air until rupture (for details see Ref. 8). The creep strain at rupture was ~4%. The sample failed in a shear-like manner, with the fracture surface plane forming an angle of ~45° to the loading axis. The fracture surface was observed with an FEI-XL30 field emission scanning electron microscope (SEM) equipped with an energy-dispersive spectrum (EDS) analyzer.

Figure 1 shows an SEM micrograph of multiple nanofibers on the fracture surface. A higher magnification micrograph is shown in the inset. The nanofibers have a more or less circular cross-section, and appear as if they were spun from a melt. Their diameter is ~250 nm, and their lengths vary from a few to over 50 μm.

Figure 2 is an SEM micrograph of another set of nanofibers, where again the diameter is ~250 nm. The lower inset magnifies the root of the nanofiber, which is reminiscent of a tree root. The upper inset shows a node in the nanofiber that became charged in the SEM as it was scanned with the electron beam at a slow scan speed, indicating that it most likely is an electric insulator.

To determine the chemistries of various features shown in Figs. 1 and 2, individual nanofibers and faceted particles were retrieved from the fracture surfaces and affixed on a conductive carbon tape for EDS analysis. Figures 3(a) and 3(b) show the EDS spectra (with SEM micrographs as insets) of a single nanofiber (a) and a faceted particle (b) taken from the fracture surface, respectively. The quantitative results from the three spectra were summarized in the respective insets in Fig. 3. Excluding the strong C signal, contributed by the carbon tape, it is obvious that the nanofiber contains high concentrations of Si and O, and negligible Ti [Fig. 3(a)]. The faceted particle, on the other hand, contains a high concentration of Ti and O and negligible Si. The reason for the higher O content recorded is not clear at this time, but could be due to the O concentration in the carbon tape adhesive. Nevertheless, on the basis of previous oxidation results,[7,11] we believe the nanofibers have an SiO_2 chemistry and the faceted particles are most probably rutile or TiO_2. The EDS spectrum in Fig. 3(c), taken on the plate-shaped grain in Fig. 2 directly on the fracture surface, indicates that the Ti_3SiC_2 grains were also oxidized.

During the first few minutes of oxidation of Ti_3SiC_2 in air at high temperatures, a thin, ~600 nm, most probably amorphous, silicon oxide layer forms.[11] Traces of this layer are sometimes found later in the oxidation process.

[a)]Address all correspondence to this author.
e-mail: z.m.sun@aist.go.jp; barsoumw@drexel.edu
DOI: 10.1557/JMR.2005.0381

In Fig. 4 we propose a possible mechanism for the formation of these nanofibers. First we assume the formation of a simple transgranular crack of a single Ti_3SiC_2 grain [Figs. 4(a) and 4(b)]. Next, a thin SiO_2 layer forms and fills the crack [Fig. 4(c)]. Upon subsequent separation of the two halves of the grain, it is not unreasonable to assume that the glassy film is drawn into fibers [Figs. 4(d) and 4(e)]. Further oxidation could then result in TiO_2 grains on the fracture surfaces that would grow with time, ultimately forming a layer on the surface (see Figs. 1 and 2).

Under such conditions, the diameters of the fibers would be determined by the thickness and viscosity of the SiO_2-based film formed on the fracture surface. This fairly uniform thickness of the nanofibers observed on the fracture surface in different locations could thus be a result of a more or less uniform thickness of this SiO_2-based film. If that is true, then it may be possible to

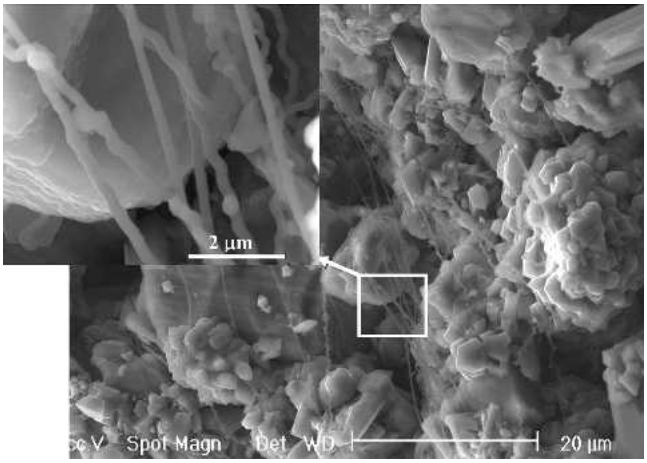

FIG. 1. Scanning electron micrograph of a Ti_3SiC_2 fracture surface after creep rupture at 1300 °C and 100 MPa, showing the nanofiber formation. Inset: details of the central part with tangled nanofibers.

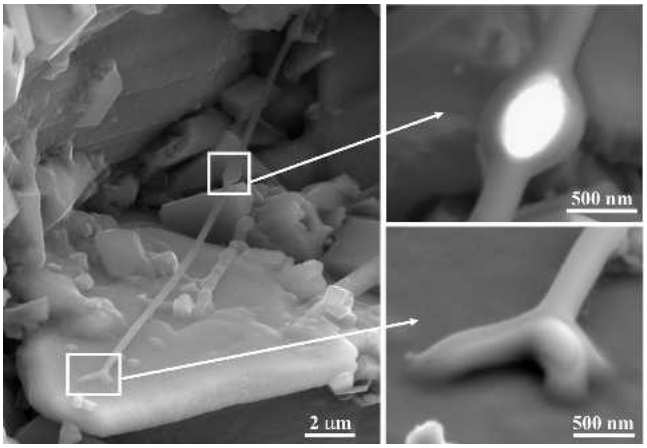

FIG. 2. A single nanofiber formed on a plate shaped grain. Insets: root of a nanofiber and a node in the middle of its length.

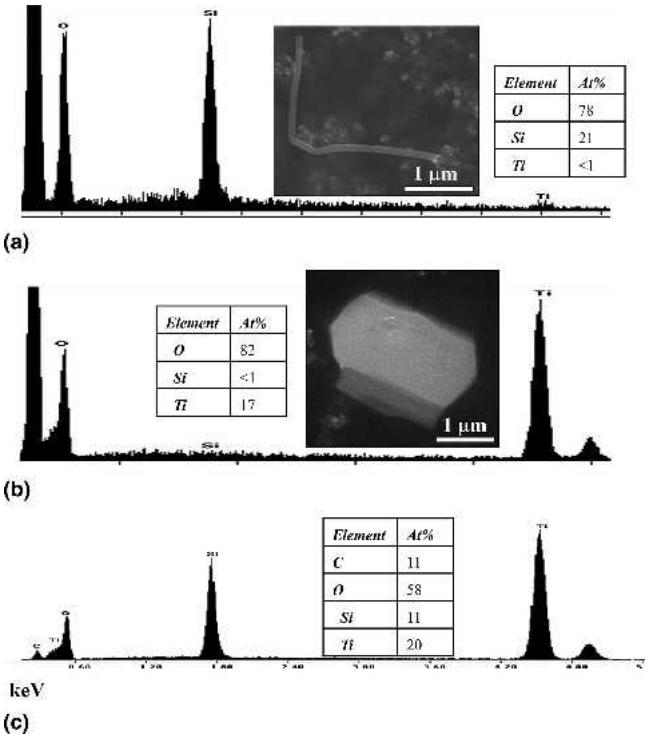

FIG. 3. (a) EDS spectrum of a single nanofiber. Inset: SEM micrograph of a nanofiber extracted from the fracture surface and placed on a conductive carbon tape. (b) EDS spectrum of a single faceted particle. Inset: SEM micrograph of a particle extracted from the fracture surface and placed on a conductive carbon tape. (c) EDS spectrum of a Ti_3SiC_2 grain on the fracture surface.

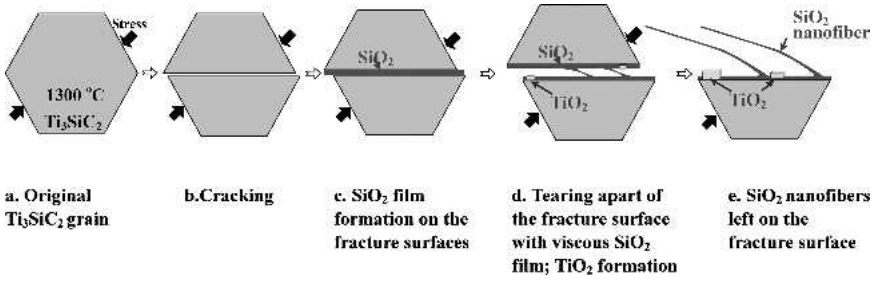

FIG. 4. Proposed mechanism for the formation of SiO_2 nanofibers.

produce different thicknesses of the nanofibers at different temperatures. The same would apply to the strain rates as well.

To estimate the depths from which Si would have to diffuse to form a typical nanofiber of, say, diameter 250 nm and length 20 μm (Fig. 2), we carried out a simple mass balance assuming the Si is coming exclusively from a plate-shaped Ti_3SiC_2 grain with dimensions of 10 μm × 10 μm × 2 μm. Assuming the fiber formed has a SiO_2 chemistry, it should consume the Si of ~16 Si basal planes. Because it has previously been shown that Si diffusion occurs preferentially along the basal planes,[12] the most likely Si path to the surface location of its oxidation is diffusion along the basal planes followed by either surface diffusion and/or evaporation condensation. These comments notwithstanding, it is hereby acknowledged that more work is needed to better understand the process by which these fibers form. At the very least, the role of O and the possible formation of SiO need to be addressed.

The significance of the results shown herein lies in their indication one more time for the selective oxidation of the A-group element in the MAX phases.

REFERENCES

1. W. Jeitschko and H. Nowotny: The crystal structure of Ti_3SiC_2—A new complex carbide. *Monatsh. Chem.* **98,** 329 (1967).
2. M.W. Barsoum: The $M_{N+1}AX_N$ phases: A new class of solids: Thermodynamically stable nanolaminates. *Prog. Solid State Chem.* **28,** 201 (2000).
3. Z.M. Sun, H. Hashimoto, Z.F. Zhang, S.L. Yang, and T. Abe: Synthesis of a metallic ceramic-Ti_3SiC_2 by PDS process and its properties, in *Solid-State Chemistry of Inorganic Materials IV,* edited by M.A. Alario-Franco, M. Greenblatt, G. Rohrer, and M.S. Whittingham (Mater. Res. Soc. Symp. Proc. **755,** Warrendale, PA, 2002), p. 179.
4. Z.M. Sun, Z.F. Zhang, H. Hashimoto, and T. Abe: Ternary compound Ti_3SiC_2. I. Pulse discharge sintering synthesis. *Mater. Trans.* **43,** 428 (2002).
5. T. Goto and T. Hirai: Chemically vapor deposited Ti_3SiC_2. *Mater. Res. Bull.* **22,** 1195 (1987).
6. J-F. Li, W. Pan, F. Sato, and R. Watanabe: Mechanical properties of polycrystalline Ti_3SiC_2 at ambient and elevated temperatures. *Acta Mater.* **49,** 937 (2001).
7. M.W. Barsoum, T. El-Raghy, and L. Ogbuji: Oxidation of Ti_3SiC_2 in air. *J. Electrochem. Soc.* **144,** 2508 (1997).
8. M.W. Barsoum, L.H. Ho-Duc, M. Radovic, and T. El-Raghy: Long time oxidation study of Ti_3SiC_2, Ti_3SiC_2/SiC and Ti_3SiC_2/TiC composites in air. *J. Electrochem. Soc.* **150,** B166 (2003).
9. M. Radovic, M.W. Barsoum, T. El-Raghy, and S.M. Wiederhorn: Tensile creep of coarse-grained Ti SiC in the 1000–1200 °C temperature range. *J. Alloys Compd.* **361,** 299 (2003).
10. T. Zhen, M.W. Barsoum, and S.R. Kalidindi: Compressive creep of Ti_3SiC_2 in the 1100 to 1300 °C temperature range in air. *Acta Mater.* (in press).
11. S.L. Yang, Z.M. Sun, and H. Hashimoto: Oxidation of Ti_3SiC_2 at 1000C in air. *Oxid. Met.* **59,** 155 (2003).
12. M.W. Barsoum, T. El-Raghy, L. Farber, M. Amer, R. Christini, and A. Adams: The topotaxial transformation of Ti_3SiC_2 to form a partially ordered cubic $TiC_{0.67}$ phase by the diffusion of Si into molten cryolite. *J. Electrochem. Soc.* **146,** 3919 (1999).